



**HAL**  
open science

# CO to Isonitrile Substitution in Iron Cyclopentadienone Complexes: A Class of Active Iron Catalysts for Borrowing Hydrogen Strategies

Gaëtan Quintil, Léa Diebold, Gibrael Fadel, Jacques Pécaut, Christian Philouze, Martin Clémancey, Geneviève Blondin, Ragnar Björnsson, Adrien Quintard, Amélie Kochem

## ► To cite this version:

Gaëtan Quintil, Léa Diebold, Gibrael Fadel, Jacques Pécaut, Christian Philouze, et al.. CO to Isonitrile Substitution in Iron Cyclopentadienone Complexes: A Class of Active Iron Catalysts for Borrowing Hydrogen Strategies. *ACS Catalysis*, 2024, 14 (10), pp.7795-7805. 10.1021/acscatal.4c01506 . hal-04590890

**HAL Id: hal-04590890**

**<https://hal.science/hal-04590890v1>**

Submitted on 14 Oct 2024

**HAL** is a multi-disciplinary open access archive for the deposit and dissemination of scientific research documents, whether they are published or not. The documents may come from teaching and research institutions in France or abroad, or from public or private research centers.

L'archive ouverte pluridisciplinaire **HAL**, est destinée au dépôt et à la diffusion de documents scientifiques de niveau recherche, publiés ou non, émanant des établissements d'enseignement et de recherche français ou étrangers, des laboratoires publics ou privés.

# CO to isonitrile substitution in iron cyclopentadienone complexes: a new class of active iron catalysts for borrowing hydrogen strategies

Gaëtan Quintil,<sup>[a,b]</sup> Léa Diebold,<sup>[b]</sup> Gibrael Fadel,<sup>[b]</sup> Jacques Pécaut,<sup>[c]</sup> Christian Philouze,<sup>[a]</sup> Martin Clémancey,<sup>[b]</sup> Geneviève Blondin,<sup>[b]</sup> Ragnar Bjornsson,<sup>[b]</sup> Adrien Quintard<sup>[a]\*</sup>, Amélie Kochem<sup>[b]\*</sup>

[a] Univ. Grenoble Alpes, CNRS, DCM, 38000 Grenoble, France.

[b] Université Grenoble Alpes, CNRS, CEA, LCBM (UMR 5249), F-38000 Grenoble, France.

[c] Univ. Grenoble Alpes, CEA, CNRS, IRIG, SYMMES F-38000 Grenoble, UMR 5819.

---

**ABSTRACT:** Discovering new active cheap iron complexes for eco-compatible borrowing hydrogen transformations constitutes a real challenge. In this context, we developed a family of isonitrile-substituted iron cyclopentadienone complexes. They were successfully applied in traditional borrowing hydrogen amine alkylation with alcohols, and notably, in the development of a photo-activated multi-catalytic enantioselective allylic alcohols functionalization. Of importance, the catalyst showing greater activity under photo-irradiation differs from the one most active in conventional amine alkylation using chemical activation. This underscores the importance of incorporating isonitrile ligands in a readily customizable manner, resulting in active catalysts with complementary reactivities. Characterization of their physical properties was complemented by DFT calculations to enhance our understanding of their behavior. Given the distinctive properties of the disclosed iron catalysts, their application is poised to pave the way for exploring challenging reactivities in related catalytic processes.

---

## INTRODUCTION

Considering sustainability and cost-efficiency, the advancement of contemporary synthetic processes should ensure minimal energy consumption, avoid stoichiometric reagents while limiting waste. In pursuit of this objective, the creation of catalyst scaffolds that promote optimal reactivity stands as a valuable aspiration. In the quest for the replacement of costly and scarce noble metal complexes, the discovery of the unique reactivities of iron cyclopentadienone catalysts in hydrogen transfer reactions has marked a significant paradigm shift.<sup>1,2</sup> Through the cooperativity between the iron metal center and the cyclopentadienone ligand, numerous efficient and selective transformations such as the eco-compatible borrowing hydrogen transformations of alcohols have been discovered.<sup>3,4</sup> In the search for improved catalyst activities, modification of the original Knölker-type complex has mainly focused on changing the cyclopentadienone core.<sup>3,5</sup> In sharp contrast, modification of the iron tricarbonyl structure has been limited, with varying success, to the insertion of phosphoramidite, phosphine or labile nitrile ligands.<sup>6</sup>

Given the crucial interactions and potential effect of ligands directly linked to the iron center, it would thus be highly desirable to explore over ligand scaffolds, which could provide iron catalysts with different complementary reactivities. These catalysts could provide improved efficiency in known reactions, and most importantly, open new avenues for the discovery of innovative reactions. In this context, we have explored the replacement of CO ligand by electronically similar isonitrile ligands.<sup>7</sup> Isonitriles are well known in

metal complexes to provide stronger  $\sigma$ -donor but weaker  $\pi$ -acceptor properties as compared to the parent CO ligand.<sup>8</sup> Of great interest as compared to CO, the diversity of potential isonitriles could enable adjusting the properties of the metal complex through the modulation of the isonitrile structures. This could lead to a family of tunable catalysts, with potential different reactivities in different conditions.

Herein, we report our success at developing such a class of iron complexes. The synthesis is straightforward and a large library of such iron complexes were synthesized and tested in borrowing hydrogen transformations. Careful and complete spectroscopic analysis of the iron complexes combined with DFT calculations, provide a better understanding of their unique properties, which should readily be applied in other catalysts design.

Most importantly, aside from reactivity in classical amine alkylation with alcohols, the unique properties of these catalysts could unlock the development of an efficient multi-catalyzed photo-induced enantioselective functionalization of allylic alcohols, providing unique activities and demonstrating their potential for future catalytic reactions discovery (Figure 1).

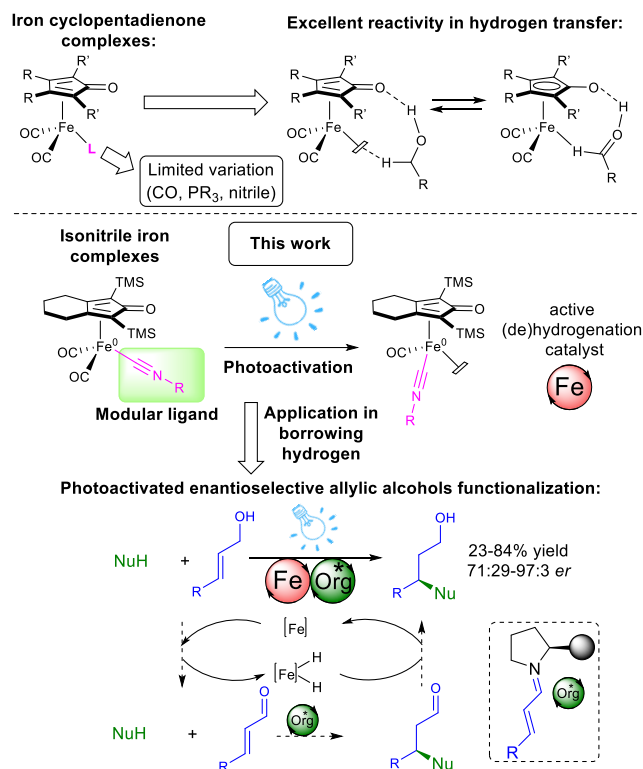


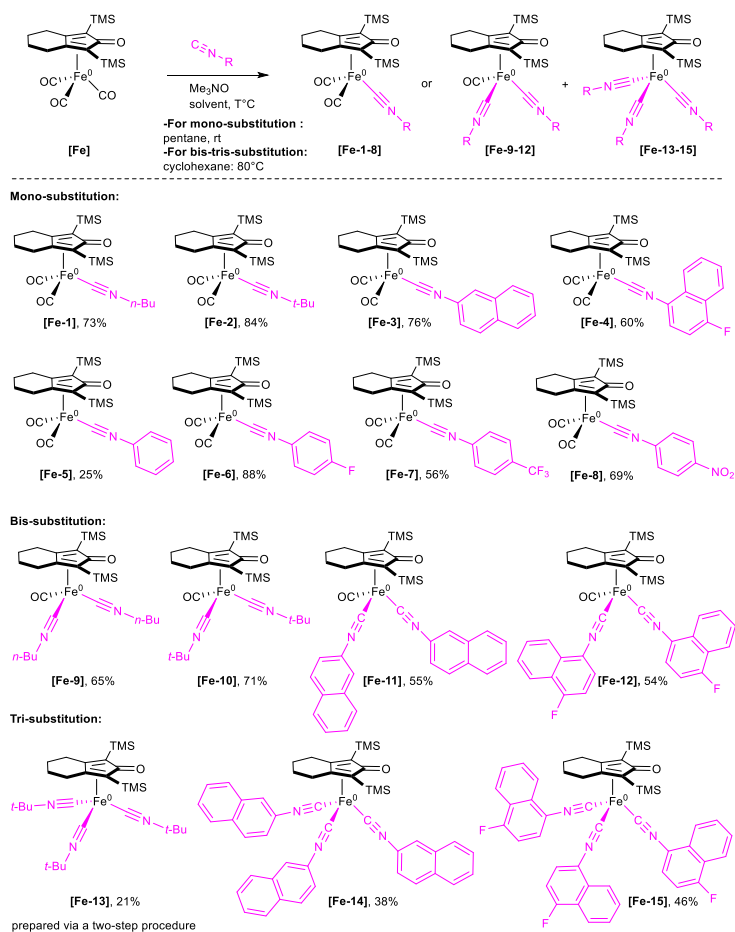
**Figure 1.** Iron cyclopentadienone and their reactivity (up). New isonitrile-substituted iron complexes and their application in the development of a photoactivated enantioselective allylic alcohols functionalization (down).

## RESULTS AND DISCUSSION

### Synthesis of iron complexes

The advantage of isonitrile-substituted iron cyclopentadienone complexes would lie in the ease of synthesis of numerous analogues featuring diversely decorated isonitrile ligands. Following the efficient two-step synthesis of the classical iron cyclopentadienone complex, simple ligand exchange would generate the desired library of potential catalysts.

We developed this strategy by condensing a wide array of isonitrile ligands, either commercially available or easily prepared,<sup>9</sup> with the tris-carbonyl complex in the presence of Me<sub>3</sub>NO (Scheme 1). The synthesis was found to be highly modular and performing the reaction at room temperature, substituted complexes **[Fe-1-8]** were easily prepared in 25 to 88% yield. They feature various substitution patterns from linear or branched aliphatic chains **[Fe-1,2]** to aromatic substituents with varying electronic patterns **[Fe-3-8]**. Forcing the reaction conditions (increasing isonitrile/Me<sub>3</sub>NO equivalents and temperature), multiple substitutions of CO could be achieved, leading to the isolation of the bis-isonitrile complexes **[Fe-9-12]** or the tris-isonitrile complexes **[Fe-13-15]**. It is interesting to note that the formation of bis- and tris-substituted complexes does not occur at room temperature but requires harsher reaction conditions. This suggests that the substitution of one CO by an isonitrile makes the corresponding mono-substituted complexes more chemically challenging to activate as compared to **[Fe]**.



**Scheme 1.** Synthesis of the isonitrile-substituted iron complexes.

### Characterization of the iron complexes and DFT correlation

With this library of iron complexes, we then studied in detail their physical properties notably corroborating different analytic techniques with DFT calculations.

All the complexes were found to bench-stable over months and stable over purification by silica gel column chromatography, demonstrating their robustness. Interestingly, these compounds were highly crystalline, and the solid structures could be determined by single-crystal XRD. Representative examples are displayed in Figure 2 (see SI for all structures). These results confirmed the structure of the obtained iron complexes and the CO to isonitrile substitutions. As compared to the classical Knölker complex **[Fe]**, the lengths of the Fe1-C17 bonds are shorter (lying at 1.77±0.01 Å for the different monosubstituted complexes vs. 1.81 Å). As compared to these Fe-CO bonds, the bond length between the iron and the different isonitriles is always about 0.1 Å longer. Of interest, while **[Fe-2]** features a *t*-Bu isonitrile substituent, the isonitrile is found to be relatively planar (176°), in complex **[Fe-8]** possessing an electron-poor aromatic, the isonitrile bent to an angle of 164° (C16-N2-C10) suggesting higher π backdonation from the iron to the isonitrile in this case. These features reflects that the CO to isonitrile substitution induces a reinforcement of the bonds between the Fe with the remaining terminal CO. These differ-

ence in bonding can be due to different  $\sigma$  and/or  $\pi$  interactions of the Fe with the surrounding ligand that were further investigated by IR spectroscopy.

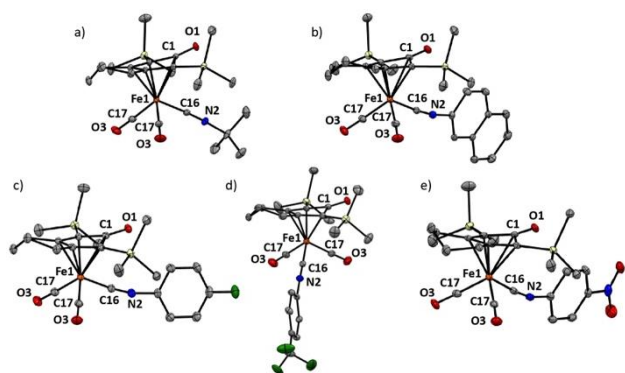


**Figure 2.** Representative solid structures by single-crystal XRD shown with 30% thermal ellipsoids and with the coordinate system used in the discussion. Color code: Fe in orange, O in red, N in blue, Si in yellow, C in grey and F in green. H atoms are omitted for clarity. a) **[Fe-2]**. b) **[Fe-3]**. c) **[Fe-6]**. d) **[Fe-7]**. e) **[Fe-8]**. See SI for structures of all complexes.

The infrared (IR) spectra of the  $\nu$ CO and  $\nu$ CN region of the powders provided important additional information concerning the complexes properties (Figure 3 and S1). The IR spectrum of **[Fe]** displays three main absorption bands in the carbonyl region at 2052, 1986 and 1604  $\text{cm}^{-1}$  (Figure 3-a). With the aid of DFT calculations, the vibrations can be assigned to the symmetric (2052  $\text{cm}^{-1}$ ) and the antisymmetric (1986  $\text{cm}^{-1}$ ) stretching frequency of the coordinated CO ligands and the stretching frequency of the cyclopentadienone CO ligand (1604  $\text{cm}^{-1}$ ). Complex **[Fe-2]** is characterized by a band at 2162  $\text{cm}^{-1}$  attributed to the CN stretching frequency, two bands attributed to the symmetric (1990  $\text{cm}^{-1}$ ) and antisymmetric (1943  $\text{cm}^{-1}$ ) stretching frequency of the terminal CO ligands and with the cyclopentadienone CO stretching frequency observed at 1591  $\text{cm}^{-1}$ . The entire series of mono-substituted complexes exhibits a consistent spectroscopic profile, with variations observed solely in the stretching frequency values. These variations are contingent upon the specific functionalizing group attached to the isonitrile.

The functionalization of the isonitrile by an aryl group instead of an alkyl group induces a shift of the CN stretching frequency at lower wavenumber (2149  $\text{cm}^{-1}$ ) in **[Fe-3]** with no effect on the CO stretching frequency. This effect is smaller with isonitrile bearing a smaller aryl group with the CN stretching frequency lying at 2157  $\text{cm}^{-1}$  in **[Fe-5]**. As compared to **[Fe-5]**, the introduction of an electro-withdrawing group in para position of the phenyl isonitrile in **[Fe-8]** induces a significant shift at lower wavenumber of the CN stretching frequency (2130  $\text{cm}^{-1}$ ) and of the CO from the cyclopentadienone ligand (1983  $\text{cm}^{-1}$ ) while the terminal CO ligands appear at higher wavenumber (1997  $\text{cm}^{-1}$  and 1958  $\text{cm}^{-1}$ ).

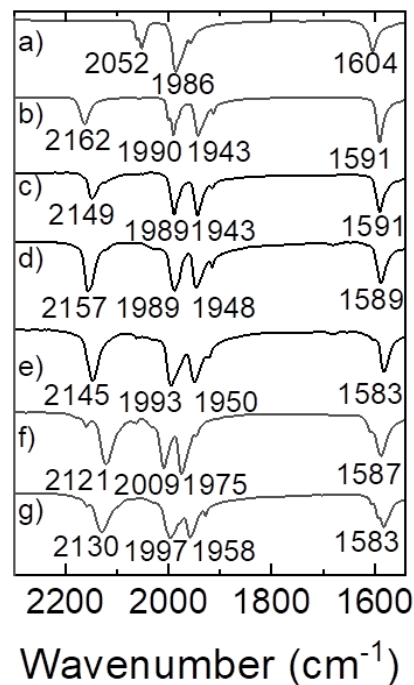


**Figure 3.** FTIR spectra in the  $\nu$ CO and the  $\nu$ CN region of powder of a) **[Fe]**. b) **[Fe-2]**. c) **[Fe-3]**. d) **[Fe-5]**. e) **[Fe-6]**. f) **[Fe-7]**. g) **[Fe-8]**. See SI for IR data of all complexes.

These observations reveal several key features. The substitution of one CO ligand by isonitrile induces a decrease of the stretching frequency of the two remaining terminal carbonyl ligands as compared to **[Fe]**. This reveals increased  $\pi$ -backdonation coming with an elongation of the C-O bonds and a shortening of the Fe-CO bonds as observed by Xray analysis of the crystalline structures. A similar trend is observed for the carbonyl of the cyclopentadienone ligand. Note that these effects are less pronounced when the isonitriles are functionalized by aryl groups bearing an electron-withdrawing group. Indeed, the **[Fe-7,8]** complexes exhibit the lowest CN stretching frequency as compared to the series of monosubstituted complexes indicated an increased  $\pi$ -backdonation. As a matter of fact, the increased Fe-CN-R  $\pi$ -backdonation comes with a decreased Fe-CO  $\pi$ -backdonation. NOCV-DFT analysis (natural orbitals for chemical valence) was performed to gain further insight into the Fe-isonitrile interactions. The calculations (see SI) reveal that the  $\sigma$  contribution to the interaction energy barely changes in the different complexes while the  $\pi$  interaction changes significantly, with the largest changes seen for **[Fe-7,8]**. Furthermore,  $\pi$ -interaction energies correlate well with the decrease in CN stretching frequency.

Bis and tris-substitution of CO by isonitriles provided the same tendency as reflected by the analysis of **[Fe-2]**, **[Fe-10]** and **Fe-13]** (Figure S1). The elongation of the remaining C-O ligand and the shortening of the Fe-CO bond is even more pronounced in **[Fe-10]** as compared to **[Fe-2]**. A linear trend is observed for the carbonyl of the cyclopentadienone ligand. The decrease of the stretching frequency corresponding to the cyclopentadienone CO ligand and concomitant elongation of the C1-O1 bond along the series of complexes **[Fe]**, **[Fe-2]**, **[Fe-10]** and **[Fe-13]** is in line with the shortening of the Fe-C1 bond in the molecular structures. When the number of substitution increases, the iron

reinforces its bonding with the remaining CO and cyclopentadienone ligands which likely explains why the chemical activation of these complexes is rendered more difficult.

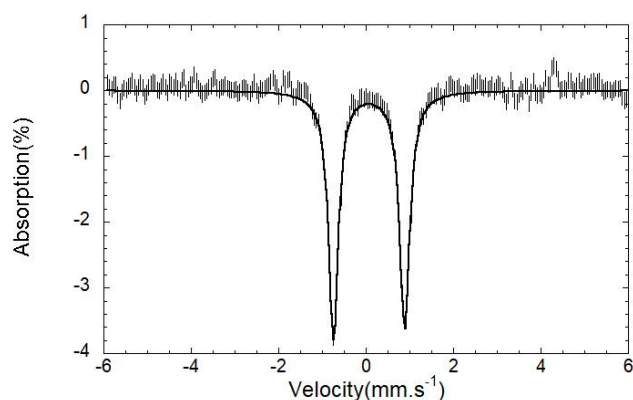


**Figure 4.** 80 K and zero-field Mössbauer spectrum (hatched bars) of powder sample of **[Fe-2]**. Simulation is shown as grey solid line.

Next, the series of monosubstituted complexes as well as the di- and tri-substituted complexes were investigated by Mössbauer spectroscopy. Their spectra recorded at 80 K, complemented by that of the tricarbonyl complex **[Fe]**,<sup>10</sup> are displayed in Figure S2-16. All the complexes are characterized by a single doublet whose nuclear parameters are listed in Table 1. It is exemplified with the spectrum of **[Fe-2]** in Figure 4. The isomer shifts and the quadrupole splittings are similar to those observed for [(diene)Fe<sup>0</sup>(CO)<sub>3</sub>] type complexes.<sup>11</sup> The monosubstituted complexes exhibit similar isomer shift of  $0.06 \pm 0.01$  mm s<sup>-1</sup> and the observed variations are below the uncertainties of the measurements ( $\pm 0.02$  mm s<sup>-1</sup> on  $\delta$ ). These results show that the substitution of one CO by an isonitrile does not have significant electronic impact on the iron center, despite the notable changes in  $\pi$  backbonding suggested by the IR analysis. Next, we examined the influence of the number of substitutions in the series of complexes **[Fe-2]**, **[Fe-10]** and **[Fe-13]** (Figure S17). Whereas the substitution of one or all CO ligands in [Fe(CO)<sub>5</sub>] by *t*-BuNC led to more negative isomer shift values,<sup>12</sup> a slight increase is observed within this series upon each substitution. This is in agreement with the better  $\sigma$ -donating character of *t*-BuNC vs CO. The ca. 0.05 mm s<sup>-1</sup> higher  $\delta$  value for **[Fe-13]** compared to that of **[Fe]** is almost identical to the increase observed between the two Fe<sup>0</sup> complexes [( $\eta^5$ -C<sub>6</sub>H<sub>7</sub>)Fe(CO)<sub>3</sub>] ( $\delta = 0.113$  mm s<sup>-1</sup> and  $\Delta E_Q = 1.55$  mm s<sup>-1</sup>)<sup>13</sup> and [( $\eta^5$ -C<sub>6</sub>H<sub>7</sub>)Fe(CN<sup>t</sup>Bu)<sub>3</sub>] ( $\delta = 0.171$  mm s<sup>-1</sup> and  $\Delta E_Q = 1.433$  mm s<sup>-1</sup>).<sup>14</sup> Moreover, the quadrupole splitting values for these two complexes are comparable to those determined within this series.

**Table 1.** Mössbauer parameters determined from simulations of spectra the mono-, di- and tri-substituted complexes. Only the absolute value of the quadrupole splitting can be experimentally determined from zero-field Mössbauer spectra. Uncertainties are  $\pm 0.02$  mm s<sup>-1</sup>,  $\pm 0.05$  mm s<sup>-1</sup> and  $\pm 0.02$  mm s<sup>-1</sup>, on  $\delta$ ,  $\Delta E_Q$  and  $\Gamma_{\text{fwhm}}$ , respectively.

| Entry | Iron complex   | $\delta$ (mm.s <sup>-1</sup> ) | $\Delta E_Q$ (mm.s <sup>-1</sup> ) | $\Gamma$ (mm.s <sup>-1</sup> ) |
|-------|----------------|--------------------------------|------------------------------------|--------------------------------|
| 1     | <b>[Fe]</b>    | 0.06                           | 1.46                               | 0.29                           |
| 2     | <b>[Fe-2]</b>  | 0.07                           | 1.63                               | 0.27/0.28                      |
| 3     | <b>[Fe-3]</b>  | 0.07                           | 1.64                               | 0.29/0.31                      |
| 4     | <b>[Fe-5]</b>  | 0.05                           | 1.68                               | 0.27                           |
| 5     | <b>[Fe-6]</b>  | 0.05                           | 1.63                               | 0.26/0.28                      |
| 6     | <b>[Fe-7]</b>  | 0.05                           | 1.60                               | 0.25/0.29                      |
| 7     | <b>[Fe-8]</b>  | 0.05                           | 1.61                               | 0.26                           |
| 8     | <b>[Fe-9]</b>  | 0.09                           | 1.63                               | 0.30/0.31                      |
| 9     | <b>[Fe-13]</b> | 0.11                           | 1.55                               | 0.30                           |

Interestingly, the UV-Vis absorption of some of the isonitrile-substituted complexes varied considerably as compared to the classical **[Fe]** complex. The UV-Vis spectra of the series of mono-substituted complexes are depicted in Figure 5 (Table 2). They are all characterized by one main absorption band located between 280 and 450 nm (although **[Fe-8]** has a shoulder). On the basis of their high intensity, these transitions are assigned to charge transfer (CT) transitions. The wavelength corresponding to the maximum absorption as well as the molar absorption coefficient vary significantly depending on the isonitrile functionalization. The spectra of **[Fe]** and **[Fe-2]** are rather similar with one main absorption band at 309 nm ( $4491$  M<sup>-1</sup>.cm<sup>-1</sup>) and 314 nm ( $5083$  M<sup>-1</sup>.cm<sup>-1</sup>), respectively.

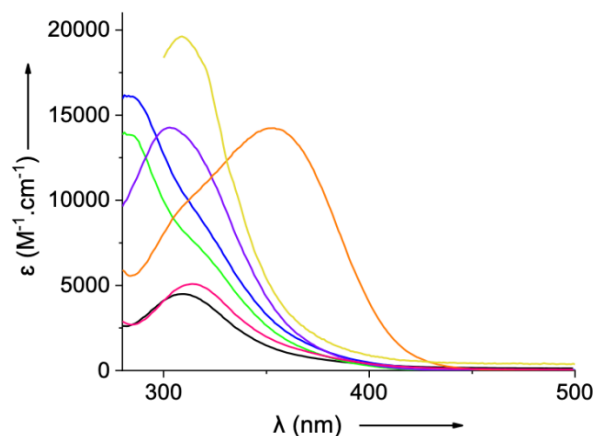


**Figure 5.** UV-visible spectra of toluene solutions of **[Fe]** (black line), **[Fe-2]** (pink line), **[Fe-3]** (yellow line), **[Fe-5]** (green line), **[Fe-6]** (blue line), **[Fe-7]** (violet line) and **[Fe-8]** (orange line). T = 298 K. See Figure S18-20 for full spectra.

**Table 2.** UV/Vis absorption spectra of the mono-substituted complexes<sup>[a]</sup>

| Entry |               | $\lambda_{\max}$<br>(nm) | $\epsilon$<br>( $M^{-1}\cdot cm^{-1}$ ) | sh <sup>[b]</sup><br>(nm) | $\epsilon$<br>( $M^{-1}\cdot cm^{-1}$ ) |
|-------|---------------|--------------------------|---|---------------------------|---|
| 1     | <b>[Fe]</b>   | 309                      | 4491                                    | -                         | -                                       |
| 2     | <b>[Fe-2]</b> | 314                      | 5083                                    | -                         | -                                       |
| 3     | <b>[Fe-3]</b> | 310                      | 19 576                                  | -                         | -                                       |
| 4     | <b>[Fe-5]</b> | 281                      | 16 176                                  | 318                       | 7 159                                   |
| 5     | <b>[Fe-6]</b> | 283                      | 13 853                                  | 320                       | 8 542                                   |
| 6     | <b>[Fe-7]</b> | 303                      | 14 274                                  | -                         | -                                       |
| 7     | <b>[Fe-8]</b> | 351                      | 14 229                                  | 308                       | 9 466                                   |

<sup>[a]</sup> Toluene solution at 298 K. <sup>[b]</sup> sh: shoulder.

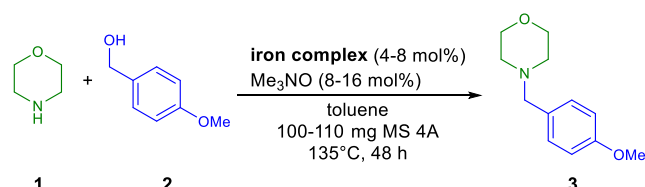
Interestingly, the mono-substituted complexes with an aryl isonitrile (naphthyl or phenyl derivative) exhibit an absorption increased by a factor of two to three as compared to **[Fe-2]**. The introduction of an electron-withdrawing atom/group in para position of the phenylisonitrile ring induces a shift of the absorption band at lower energy (281 nm ( $16\,176\,M^{-1}\,cm^{-1}$ ), 283 nm ( $13\,853\,M^{-1}\,cm^{-1}$ ), 303 nm ( $14\,274\,M^{-1}\,cm^{-1}$ ) and 351 nm ( $14\,229\,M^{-1}\,cm^{-1}$ ) for **[Fe-5]**, **[Fe-6]**, **[Fe-7]** and **[Fe-8]**, respectively). Thus, this tendency directly correlates with the electron-withdrawing character of this atom/group and could have interesting implications in catalysis under photoactivation.

### Application in borrowing hydrogen

Initial attempts at using the newly designed catalyst in borrowing hydrogen such as in the classical amine alkylation using alcohols, confirmed their catalytic activities (Table 3, see Table S11 for full details). Using 4 mol% of the iron complex, conversion to the alkylated amines occurred in 26-59% yield using the mono-alkylated isonitrile complexes (entries 2-8), while **[Fe]** provided a quantitative yield under the same conditions (entry 1). More bulky **[Fe-2]** and electron-rich **[Fe-3]** provided the lower conversion (entries 3-4) while electron-poor isonitrile ligands provided the best results (entries 5-8). Di-substituting the iron centre with two isonitriles ligands decreased the reactivity (entries 10-11).

To underscore the potential of these novel complexes, we were enthusiastic about testing them in more demanding transformations. Most notably, given the light-absorption properties of the newly synthesized complexes, different to the classical Knölker complex, we hypothesized that interesting properties could be achieved in reactions taking advantage of light for activation of the iron complex.<sup>15</sup> Our group disclosed the enantioselective functionalization of allylic alcohols based on the combination between a metal catalyst for the borrowing hydrogen and a chiral iminium-type organocatalyst for the enantioselective nucleophilic addition on the transient catalytically generated  $\alpha,\beta$ -unsaturated aldehyde.<sup>16</sup> These reactions, using  $Me_3NO$  as metal-complex activating reagent, were problematic concerning the compatibility with acidic functions. Indeed, it

has been shown that the chemical activation of the precatalyst leads to the formation of  $[LFe(CO)_2(NMe_3)]$  type species, by releasing the trimethylamine base in solution to generate the active species  $[LFe(CO)_2]$ .<sup>17</sup> However, initial attempts at avoiding the use of  $Me_3NO$  activation through photoactivation, required lights with low wavelengths, providing moderate yield (47%), due to the partial decomposition of the iron complex under strong UV irradiation while this also resulted in moderate *ee* (69%).<sup>3b</sup> Since an interesting bathochromic shift was observed in the light absorption spectra with some of the complexes, it would thus be possible to perform with greater efficiency the multicatalytic borrowing hydrogen using substrate tolerant and less energetic LED light sources that are more common and available.

**Table 3.** UV/ Selected iron complexes activity in amine alkylation.

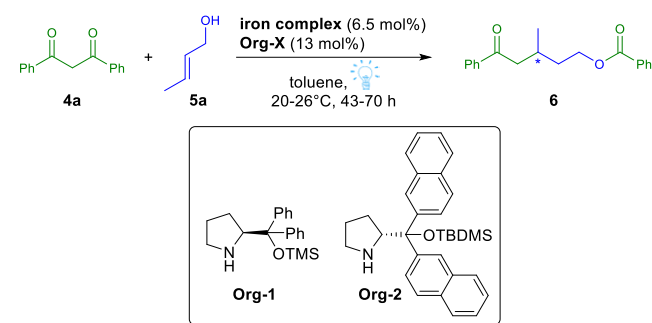
| Entry | Iron complex   | Yield <sup>[a]</sup> |
|-------|----------------|----------------------|
| 1     | <b>[Fe]</b>    | 99%                  |
| 2     | <b>[Fe-1]</b>  | 41%                  |
| 3     | <b>[Fe-2]</b>  | 26%                  |
| 4     | <b>[Fe-3]</b>  | 32%                  |
| 5     | <b>[Fe-4]</b>  | 54%                  |
| 6     | <b>[Fe-6]</b>  | 59%                  |
| 7     | <b>[Fe-7]</b>  | 53%                  |
| 8     | <b>[Fe-8]</b>  | 39%                  |
| 9     | <b>[Fe-10]</b> | 7%                   |
| 10    | <b>[Fe-11]</b> | 26%                  |

<sup>[a]</sup> Determined by <sup>1</sup>H NMR using dibromomethane as internal standard.

In order to develop such reactivity, we screened the classical Knölker complex and the isonitrile-substituted complexes in the condensation of dibenzoylmethane **4a** to allylic alcohol **5a** using **Org-1** and 368 nm LED photoactivation (Table 4). Upon functionalization of the allylic alcohol, the obtained chiral aliphatic alcohol spontaneously rearranges through Claisen fragmentation to generate **6** featuring a mono-ketone and an ester.<sup>3b</sup> Under those conditions, the classical iron complex **[Fe]** only provided 9% conversion (entry 1). Alkyl-isonitrile complexes also did not prove sat-

isfying, without any noticeable conversion to the functionalized alcohol (entry 2). Aromatic-substituted nitriles provided improved reactivity furnishing 17-56% conversion for **[Fe-3,4,6,7]** (entries 3-5). Gratifyingly, **[Fe-8]** was optimal in this transformation, affording the borrowing hydrogen cascade adduct in 93% conversion and 74:26 *er* (entry 8). Finally, disubstituted and trisubstituted iron complexes **[Fe-9-15]** only provided trace conversion to the desired product (entry 9). From these experiments, the reactivity follows the trend observed in light-absorption (Figure 5), with the nitro-aromatic isonitrile complex with the higher bathochromic shift being the only one able to efficiently harness the energy from the light source to provide the desired reactivity. Of interest, it must be pointed out that the catalyst the more active under photo-irradiation is not the most active in classical amine alkylation under chemical activation. This highlights the interest of this strategy of incorporating isonitrile ligands in an easily modular manner which leads to active catalysts with complementary reactivities. Further optimization of the reaction (see SI for details), using bulkier **Org-2** under more concentrated conditions, afforded **6** in 79% isolated yield and 86:14 *er* (entries 10-11).

**Table 4.** Selected iron complexes activity in the photo-induced enantioselective functionalization of allylic alcohols.



| Entry             | Iron complex     | Org          | Conversion <sup>[a]</sup> | Yield <sup>[b]</sup> | <i>er</i> <sup>[c]</sup> |
|-------------------|------------------|--------------|---------------------------|----------------------|--------------------------|
| 1                 | <b>[Fe]</b>      | <b>Org-1</b> | 9%                        | nd                   | nd                       |
| 2                 | <b>[Fe-1-2]</b>  | <b>Org-1</b> | <5%                       | nd                   | nd                       |
| 3                 | <b>[Fe-3]</b>    | <b>Org-1</b> | 36%                       | 29%                  | 72:28                    |
| 4                 | <b>[Fe-4]</b>    | <b>Org-1</b> | 56%                       | 42%                  | 72:28                    |
| 6                 | <b>[Fe-6]</b>    | <b>Org-1</b> | 35%                       | 29%                  | 70:10                    |
| 7                 | <b>[Fe-7]</b>    | <b>Org-1</b> | 17%                       | nd                   | nd                       |
| 8                 | <b>[Fe-8]</b>    | <b>Org-1</b> | 93%                       | 81%                  | 74:26                    |
| 9                 | <b>[Fe-9-15]</b> | <b>Org-1</b> | <6%                       | nd                   | nd                       |
| 10                | <b>[Fe-8]</b>    | <b>Org-2</b> | 76%                       | 67%                  | 88:12                    |
| 11 <sup>[d]</sup> | <b>[Fe-8]</b>    | <b>Org-2</b> | >95%                      | 79%                  | 86:14                    |

Reactions performed using 0.2 mmol of diketone, 0.4 mmol of allyl alcohol in 0.65 mL of toluene. <sup>[a]</sup> Determined by <sup>1</sup>H NMR. <sup>[b]</sup> Isolated yield. <sup>[c]</sup> Determined by SFC. <sup>[d]</sup> Reaction

performed under more concentrated conditions (0.325 mL of toluene). nd: not determined

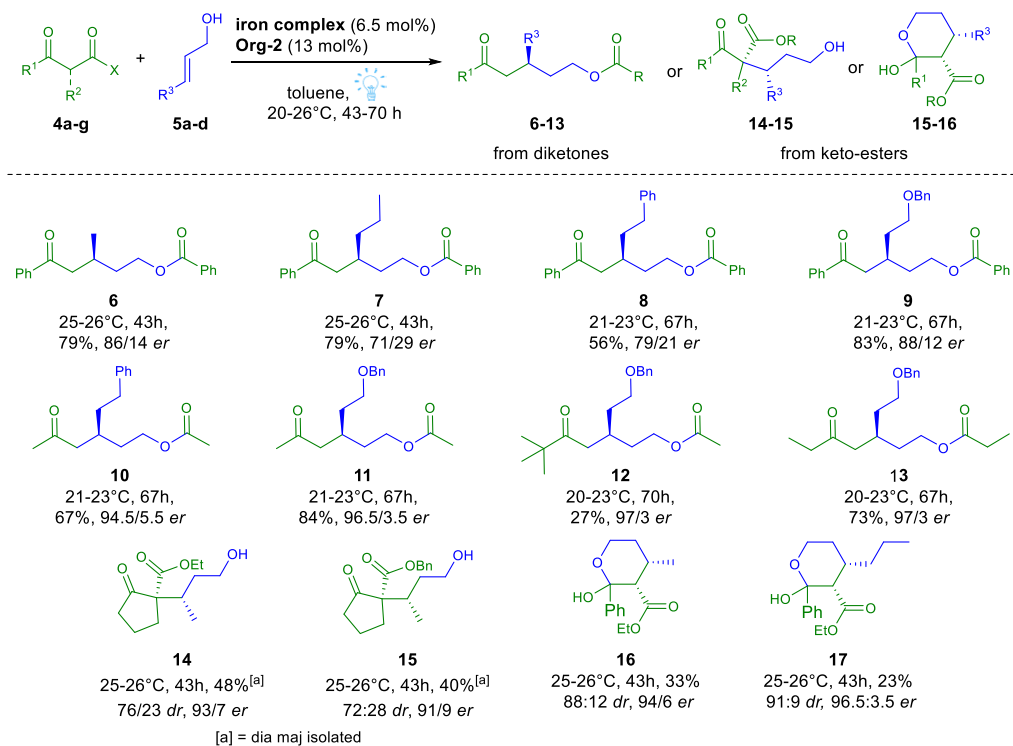
With the optimized catalysts in hand, we then tested a selection of different pro-nucleophiles and allylic alcohols under the optimized conditions (Scheme 2). Using dibenzoyl methane and different allylic alcohols, the corresponding cascade adducts **6-9** were isolated in excellent yields (56-83%) and 71:29 to 88:12 *er*. This highlights the excellent reactivity achieved by the new iron complex in reversible hydrogen transfer. All the other used pro-nucleophiles, provided the expected products in higher enantiocontrol (91:9 to 97:3 *er*), independently of the role of the iron complex. Using acetylacetone on functionalized allylic alcohols, the borrowing hydrogen adducts **10-11** were generated in 67-84% yield and 94.5:5.5-96.5:3.5 *er*. Substituted diketones lead to products **12-13** in excellent 97:3 *er* and 27-73% yield, the bulkier ketone providing lower reactivity during the iminium type addition. From substituted keto-esters, the reactivity of the catalytic system was excellent and **14-15** were formed in 91:9-93:7 *er* and 40-48% yield for the isolated major diastereomers. Acyclic keto-ester also worked well, with the products **16-17** isolated in 94:6-96.5:3.5 *er*, even though the yields were lower due to purification issue and reduction of the ketone adduct.

Altogether, these examples demonstrate the efficiency of the iron complex **[Fe-8]** under photo-activation, to provide excellent reactivity in the functionalization of allylic alcohols, improving the potential of such approach. This should lead to further discoveries in photo-induced borrowing hydrogen.

### Understanding the correlation between isonitrile functionalization and reactivity

In order to better understand this reactivity under photo-activation and confirm the role of the isonitrile ligand, different control experiments were performed and the spectroscopic data and reactivity correlated with DFT calculations. Mechanistically, photoactivation could lead to two different activation pathways. Either, the photoirradiation leads to dissociation of the isonitrile, which could stay in solution being able re-coordinate to the iron, limiting the degradation of the catalyst. Alternatively, photoirradiation leads to dissociation, providing an active iron catalyst featuring the coordinated isonitrile ligand.

A control experiment irradiating at 368 nm **[Fe-8]** in the presence of a stabilizing exogenous PPh<sub>3</sub> ligand, lead to the formation of a mixture of unreacted **[Fe-8]** (27%) and a new species **[Fe-16]** in 60% isolated yield which could be characterized by XRD (Figure 6) and NMR (see SI). Analysis of the structure reveals that one terminal CO had been substituted by one PPh<sub>3</sub> ligand. Calculations confirm that the substitution of one CO ligand by PPh<sub>3</sub> is ~4 kcal/mol favorable than substitution of the isonitrile ligand. These results thus strongly suggest the decoordination of one terminal CO to occur under irradiation and the generation of an activated species whose structure differs from the classical [FeL(CO)<sub>2</sub>]. An identical experiment was conducted with complex **[Fe-2]**, leading to similar results with the formation of the complex **[Fe-17]** (see SI) in which one CO ligand was replaced by PPh<sub>3</sub>. Compared to the experiment conducted with **[Fe-8]**, the yield is lower (28 % isolated yield



**Scheme 2.** Scope of the photo-activated multicatalytic borrowing hydrogen

and 48% of unreacted starting mat), and a significant amount of unidentified degradation products is observed. These results suggest that the photoactivation is facilitated in the case of complex **[Fe-8]** bearing an aryl isonitrile with an electron-withdrawing group over **[Fe-2]** bearing an alkyl one, and might furthermore be correlated to the higher catalytic activity of **[Fe-8]**.

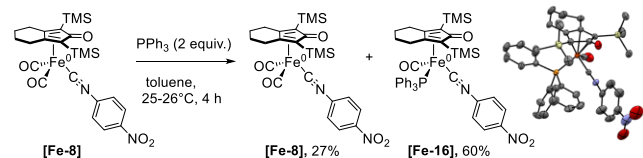


**Figure 6.** Irradiation of **[Fe-8]** in the presence of exogenous  $\text{PPh}_3$  ligand and X-ray structure of the new species formed.

Comparing the absorption spectra in Figure 5, **[Fe-8]** stands out amongst the mono-substituted series of complexes, having absorption at the lowest energy. Interestingly, the  $\lambda_{\text{max}}$  is almost identical to the wavelength used for the photocatalytic reactions where **[Fe-8]** shows the highest catalytic activity. As a result, photo-irradiation would favor the photo-excitation of this complex and the transfer of energy leading to the CO decoordination.

The nature of the CT transitions was investigated by time-dependent DFT (TD-DFT) calculations. For the 5 complexes in Figure 5 the UV-VIS spectra could be well reproduced (see SI). Analyzing the calculated spectrum of **[Fe]** using difference density analysis we find that the primary transitions at 4.2 eV (~290 nm) can be well described as metal-to-ligand charge transfer (MLCT) excitations from occupied Fe 3d orbitals to CO  $\pi^*$  orbitals. The transitions for **[Fe-2]** are analogous, with transitions into CN  $\pi^*$  orbitals as well.

The same type of transitions in the 4.2 eV region are also found to be present in **[Fe-8]** with increased intensity and

some contribution from the CN  $\pi^*$  orbitals. However, the primary difference between **[Fe-8]** and the other compounds arises from 2 intense transitions in the 3.5-3.7 eV region. These transitions can be described as Fe 3d  $\rightarrow$  isonitrile ligand  $\pi^*$  charge-transfer excitations (MLCT) with a significant contribution from the  $\text{NO}_2$  group of the ligand.

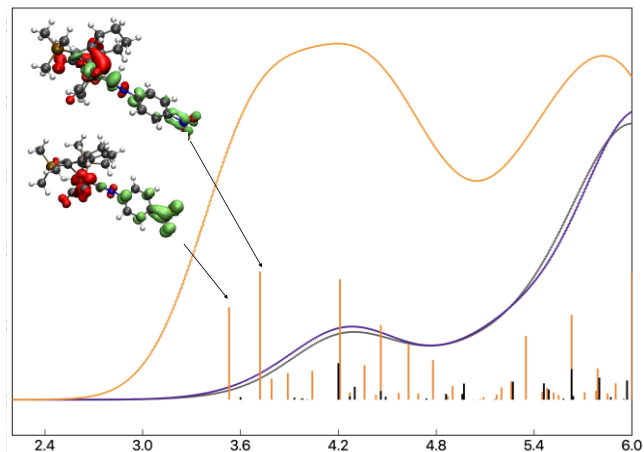


**Figure 7.** Comparison of the TD-DFT calculated spectra of **[Fe]** (gray), **[Fe-2]** (purple) with **[Fe-8]** (orange). Difference densities for the indicated transitions are shown, revealing the character behind the transition (red corresponds to density decrease and green to density increase).

The low-energy shifted absorption properties of **[Fe-8]** compared to the other isonitrile complexes **[Fe-2-7]** appears to be related to the presence of the  $\text{NO}_2$  group on the phenylisonitrile ligand. The MO diagram of **[Fe-8]** shows that it features a specific low-lying  $\pi^*$  orbital (as the LUMO) which is effectively introduced by the  $\text{NO}_2$  group (confirmed by individual ligand calculation) that mixes with the phenyl- and -CN group  $\pi^*$  orbitals. Comparative MO diagrams



of complexes and individual ligands and LUMO isosurfaces are found in the SI. Mixing of the  $\pi^*$  NO<sub>2</sub> orbitals with the phenyl ring and CN group likely also explains the improved Fe-CN-R  $\pi$ -backdonation in **[Fe-8]** compared to **[Fe-5]**.

The unique electronic structure features of **[Fe-8]** can hence be explained well by the -NO<sub>2</sub> group in the phenyl-para position mixing with the  $\pi$ -system of the phenylisonitrile ligand, creating the conditions for an intense MLCT transition. As shown in the SI, moving the -NO<sub>2</sub> group to the ortho or meta positions shifts the transition to higher energies as well as reducing the intensity. This suggests improved  $\pi$ -overlap within the ligand to be an important factor in the absorption process. Calculations were also used to investigate the removal of either CO or CN-R from **[Fe-8]**, to generate the 16-electron species [CpFe(CO)(CN-R)] or [CpFe(CO)<sub>2</sub>]. Removal of the CO ligand is favored by ~2.5 kcal/mol over the decoordination of the isonitrile ligand.

Generation of a new active [LFe(CO)(CN-R)] type species (instead of [FeL(CO)<sub>2</sub>]) with differing isonitrile ligands could hence explain the different catalytic behavior of the monosubstituted isonitrile complexes over the Knölker complex. However, preliminary mechanistic calculations of alcohol oxidation (shown in the SI) do not suggest the isonitrile ligands to significantly affect the reaction profiles. Additionally, as the Mössbauer studies indicated, the electronic modulation at the Fe center by the isonitrile ligand is actually mild, if negligible. Instead, we suggest that the increased reactivity of **[Fe-8]** is more likely rooted in the nature of the absorption and photoactivation itself. A pre-catalyst with increased absorption at the irradiation wavelength should more easily generate the active 16-electron active species [CpFe(CO)(CN-R)] which can then promptly dehydrogenate the alcohol substrate. Further studies regarding the nature of the activation mechanism are undergoing in our laboratory.

## CONCLUSION

To conclude, a family of various isonitriles-substituted iron cyclopentadienone complexes was efficiently prepared. Characterization of their physical properties was coupled with DFT calculations to better understand their behavior. This led to successful application in classical borrowing hydrogen amine alkylation with alcohols and most importantly, in the development of a photo-activated multicyclic enantioselective allylic alcohols functionalization. The newly designed iron complexes provided much higher reactivity than classical ones in these transformations. It is noteworthy to emphasize that the catalyst exhibiting higher activity under photo-irradiation differs from the one most active in conventional amine alkylation using chemical activation. This underscores the significance of incorporating isonitrile ligands in a readily customizable manner, resulting in active catalysts with complementary reactivities. Further tuning of the isonitrile ligands should also lead in the future to iron complexes activable under visible light. Given the unique properties of the disclosed iron catalysts, their application should open a new era for the discovery of challenging reactivities in related catalytic processes.

## ASSOCIATED CONTENT

Experimental protocols, detailed analysis, additional optimization experiments. This material is available free of charge via the Internet at <http://pubs.acs.org>.

## AUTHOR INFORMATION

### Corresponding Authors

Adrien Quintard

Univ. Grenoble Alpes, CNRS, DCM, 38000 Grenoble, France  
orcid.org/0000-0003-0193-6524

Email : [adrien.quintard@univ-grenoble-alpes.fr](mailto:adrien.quintard@univ-grenoble-alpes.fr)

Amélie Kochem

Université Grenoble Alpes, CNRS, CEA, LCBM (UMR 5249), F-38000 Grenoble, France.

Email : [amelie.kochem@cea.fr](mailto:amelie.kochem@cea.fr)

### Authors

Gaëtan Quintil

Univ. Grenoble Alpes, CNRS, DCM, 38000 Grenoble, France  
Léa Diebold

Université Grenoble Alpes, CNRS, CEA, LCBM (UMR 5249), F-38000 Grenoble, France

Jacques Pécaut

Univ. Grenoble Alpes, CEA, CNRS, IRIG, SYMMES F-38000 Grenoble, UMR 5819

Martin Clémancey

Université Grenoble Alpes, CNRS, CEA, LCBM (UMR 5249), F-38000 Grenoble, France

Geneviève Blondin

Université Grenoble Alpes, CNRS, CEA, LCBM (UMR 5249), F-38000 Grenoble, France

Gibrael Fadel

Université Grenoble Alpes, CNRS, CEA, LCBM (UMR 5249), F-38000 Grenoble, France

Ragnar Björnsson

Université Grenoble Alpes, CNRS, CEA, LCBM (UMR 5249), F-38000 Grenoble, France

### Author Contributions

The manuscript was written through contributions of all authors. All authors have given approval to the final version of the manuscript.

### Funding Sources

The Centre National de la Recherche Scientifique (CNRS), Université Grenoble-Alpes, the Commissariat à l'énergie Atomique, the Agence Nationale de la Recherche (ANR-23-CE07-0043) the Labex ARCANE and CBH-EUR-GS (ANR-17-EURE-0003) are warmly acknowledged for financial support.

## ACKNOWLEDGMENT

Anestis Alexandridis is greatly acknowledged for assembling the photoreactor.

## REFERENCES

- (1) For initial discoveries in hydrogenation and hydrogen transfer, see: a) Casey, C. P.; Guan, H. An Efficient and Chemoselective Iron Catalyst for the Hydrogenation of Ketones. *J. Am. Chem. Soc.* **2007**, *129*, 5816 – 5817; e) Casey, C. P.; Guan, H. Cyclopentadi-

- enone Iron Alcohol Complexes: Synthesis, Reactivity, and Implications for the Mechanism of Iron-Catalyzed Hydrogenation of Aldehydes. *J. Am. Chem. Soc.* **2009**, *131*, 2499–2507.
- (2) For reviews, see: a) Quintard, A.; Rodriguez, J. Iron Cyclopentadienone Complexes: Discovery, Properties, and Catalytic Reactivity. *Angew. Chem. Int. Ed.* **2014**, *53*, 4044; b) Quintard, A.; Rodriguez, J. A Step into an eco-Compatible Future: Iron- and Cobalt catalyzed Borrowing Hydrogen Transformation. *ChemSusChem*. **2016**, *9*, 28; c) Pignataro, L.; Gennari, C. Recent Catalytic Applications of (Cyclopentadienone)iron Complexes. *Eur. J. Org. Chem.* **2020**, 3192; d) Akter, M.; Anbarasan, P. (Cyclopentadienone)iron Complexes: Synthesis, Mechanism and Applications in Organic Synthesis. *Chem Asian J.* **2021**, *16*, 1703–1724.
- (3) For examples of borrowing hydrogen reactions using iron cyclopentadienone complexes, see: a) Quintard, A.; Constantieux, T.; Rodriguez, J. An Iron/Amine-Catalyzed Cascade Process for the Enantioselective Functionalization of Allylic Alcohols. *Angew. Chem. Int. Ed.* **2013**, *52*, 12883–12887; b) Roudier, M.; Constantieux, T.; Quintard, A.; Rodriguez, J. Enantioselective Cascade Formal Reductive Insertion of Allylic Alcohols into the C(O)–C Bond of 1,3-Diketones: Ready Access to Synthetically Valuable 3-Alkylpentanol Units. *Org. Lett.* **2014**, *16*, 2802–2805; c) Yan, T.; Feringa, B. L.; Barta, K. Iron catalyzed direct alkylation of amines with alcohols. *Nature Communications*, **2014**, *5*, 5602–5608; d) Elangovan, S.; Sortais, J.-B.; Beller, M.; Darcel, C. Iron-Catalyzed  $\alpha$ -Alkylation of Ketones with Alcohols. *Angew. Chem. Int. Ed.* **2015**, *54*, 14483–14486; e) Pan, H.-J.; Nga, T. W.; Zhao, Y. Iron-catalyzed amination of alcohols assisted by Lewis acid. *Chem. Commun.* **2015**, *51*, 11907–11910; f) Rawlings, A. J.; Diorazio, L. J.; Wills, M. C–N Bond Formation between Alcohols and Amines Using an Iron Cyclopentadienone Catalyst. *Org. Lett.* **2015**, *17*, 1086–1089; g) Roudier, M.; Constantieux, T.; Quintard, A.; Rodriguez, J. Triple Iron/Copper/Iminium Activation for the Efficient Redox Neutral Catalytic Enantioselective Functionalization of Allylic Alcohols. *ACS Catal.* **2016**, *6*, 5236–5244; h) Seck, C.; Diagne Mbaye, M.; Gaillard, S.; Renaud, J.-L. Bifunctional Iron Complexes Catalyzed Alkylation of Indoles. *Adv. Synth. Catal.* **2018**, *360*, 4640–4645; i) Lator, A.; Gaillard, S.; Poater, A.; Renaud, J.-L. Well-Defined Phosphine-Free Iron-Catalyzed N-Ethylation and N-Methylation of Amines with Ethanol and Methanol. *Org. Lett.* **2018**, *20*, 5985–5990; j) Polidano, K.; Allen, B. D. W.; Williams, J. M. J.; Morrill, L. C. Iron-Catalyzed Methylation Using the Borrowing Hydrogen Approach. *ACS Catal.* **2018**, *8*, 6440–6445; k) Quintard, A.; Roudier, M.; Rodriguez, J. Multicatalytic Enantioselective Borrowing Hydrogen  $\delta$ -Lactonization Strategy from  $\beta$ -Keto Esters and Allylic Alcohols. *Synthesis*. **2018**, *50*, 785–792; l) Latham, D. E.; Polidano, K.; Williams, J. M. J.; Morrill, L. C. One-Pot Conversion of Allylic Alcohols to  $\alpha$ -Methyl Ketones via Iron-Catalyzed Isomerization–Methylation. *Org. Lett.* **2019**, *21*, 7914–7918; m) Bettoni, L.; Gaillard, S.; Renaud, J.-L. Iron-Catalyzed  $\beta$ -Alkylation of Alcohols. *Org. Lett.* **2019**, *21*, 8404–8408; n) Bettoni, L.; Gaillard, S.; Renaud, J.-L. Iron-Catalyzed  $\alpha$ -Alkylation of Ketones with Secondary Alcohols: Access to  $\beta$ -Disubstituted Carbonyl Compounds. *Org. Lett.* **2020**, *22*, 2064–2069.
- (4) For selected reviews on borrowing hydrogen, see: a) Gunanathan, C.; Milstein, D. Applications of Acceptorless Dehydrogenation and Related Transformations in Chemical Synthesis. *Science* **2013**, *341*, 1229712–1229724; b) Quintard, A.; Rodriguez, J. Catalytic enantioselective OFF-ON activation processes initiated by hydrogen transfer: concepts and challenges. *Chem. Commun.* **2016**, *52*, 10456–10473; c) Reed-Berendt, B. G.; Polidano, K.; Morrill, L. C. *Org. Biomol. Chem.* **2019**, *17*, 1595; d) Reed-Berendt, B. G.; Latham, D. E.; Dambatta, M. B.; Morrill, L. C. Borrowing Hydrogen for Organic Synthesis. *ACS Cent. Sci.* **2021**, *7*, 570–585.
- (5) a) Knölker, H.-J.; Heber, J.; Mahler, C. H. Transition Metal-Diene Complexes in Organic Synthesis, Part 14.1 Regioselective Iron-Mediated [2+2+1] Cycloadditions of Alkynes and Carbon Monoxide: Synthesis of Substituted Cyclopentadienones. *Synlett* **1992**, *12*, 1002–1004; b) Pearson, A. J.; Shively, Jr. R. J.; Dubbert, R. A. Iron Carbonyl Promoted Conversion of  $\alpha,\omega$ -Dienes to (Cyclopentadienone) iron Complexes. *Organometallics* **1992**, *11*, 4096–4104; c) Knölker, H.-J.; Heber, J. Transition Metal-Diene Complexes in Organic Synthesis, Part 18.1 Iron-Mediated [2+2+1] Cycloadditions of Dienes and Carbon Monoxide: Selective Demetalation Reactions. *Synlett* **1993**, *12*, 924–926; d) Moyer, S. A.; Funk, T. W. Air-stable iron catalyst for the Oppenauer-type oxidation of alcohols. *Tetrahedron Letters*, **2010**, *51*, 5430–5433; e) Mérel, D. S.; Elie, M.; Lohier, J.-F.; Gaillard, S.; Renaud, J.-L. Bifunctional Iron Complexes: Efficient Catalysts for C=O and C=N Reduction in Water. *ChemCatChem* **2013**, *5*, 2939–2945; f) Moulin, S.; Dentel, H.; Pagnoux-Ozherelyeva, A.; Gaillard, S.; Poater, A.; Cavallo, L.; Lohier, J.-F.; Renaud, J.-L. Bifunctional (Cyclopentadienone)Iron–Tricarbonyl Complexes: Synthesis, Computational Studies and Application in Reductive Amination. *Chem. Eur. J.* **2013**, *19*, 17881–17890; g) Thai, T.-T.; Mérel, D. S.; Poater, A.; Gaillard, S.; Renaud, J.-L. Highly Active Phosphine-Free Bifunctional Iron Complex for Hydrogenation of Bicarbonate and Reductive Amination. *Chem. Eur. J.* **2015**, *21*, 7066–7070; h) Vailati Facchini, S.; Neudörfl, J.-M.; Pignataro, L.; Cettolin, M.; Gennari, C.; Berkessel, A.; Piarullia, U. Synthesis of [bis(hexamethylene)cyclopentadienone]iron tricarbonyl and its application to catalytic reductions of C=O. *ChemCatChem*. **2017**, *9*, 1461–1468; i) Gaignard Gaillard, Q.; Bettoni, L.; Paris, D.; Lequertier, C.; Lohier, J.-F.; Gaillard, S.; Renaud, J.-L. Synthesis of Triaminocyclopentadienyl Iron(II) Tricarbonyl Complexes and Application to the Synthesis of Aminophosphines. *Adv. Synth. Catal.* **2023**, *365*, 3704–3712.
- (6) Ref 1b and: a) Berkessel, A.; Reichau, S.; von der Höh, A.; Leconte, N.; Neudörfl, J.-M. Light-Induced Enantioselective Hydrogenation Using Chiral Derivatives of Casey's Iron–Cyclopentadienone Catalyst. *Organometallics* **2011**, *30*, 3880–3887; b) Plank, T. N.; Drake, J. L.; Kim, D. K.; Funk, T. W. Air-Stable, Nitrile-Ligated (Cyclopentadienone)iron Dicarboxyl Compounds as Transfer Reduction and Oxidation Catalysts. *Adv. Synth. Catal.* **2012**, *354*, 597–601; c) Elangovan, S.; Quintero-Duque, S.; Dorcet, V.; Roisnel, T.; Norel, L.; Darcel, C.; Sortais, J.-B. Knölker-Type Iron Complexes Bearing an N-Heterocyclic Carbene Ligand: Synthesis, Characterization, and Catalytic Dehydration of Primary Amides. *Organometallics* **2015**, *34*, 4521–4528.
- (7) For selected reviews on isonitriles complexes, see: Mukhopadhyay, S.; Patro, A. G.; Vadavi, R. S.; Nembenna, S. Coordination Chemistry of Main Group Metals with Organic Isonitriles. *Eur. J. Inorg. Chem.* **2022**, 2022; b) Boyarskiy, V. P.; Bokach, N. A.; Luzyanin, K. V.; Kukushkin, V. Y. Metal-Mediated and Metal-Catalyzed Reactions of Isonitriles. *Chem. Rev.* **2015**, *115*, 2698–2779; c) Knorn, M.; Lutsker, E.; Reiser, O. Isonitriles as Supporting and Non-Innocent Ligands in Metal Catalysis. *Chem. Soc. Rev.* **2020**, *49*, 7730–7752; d) Fehlhammer, W. P.; Fritz, M. Emergence of a CNH and Cyano Complex Based Organometallic Chemistry. *Chem. Rev.* **1993**, *93* (3), 1243–1280.
- (8) For examples of iron-isonitrile complexes efficient for transfer hydrogenation and dehydrogenative coupling of alcohols, see: a) Nguyen, D. H.; Merle, D.; Merle, N.; Trivelli, X.; Capet, F.; Gauvin, R. M. Isonitrile Ruthenium and Iron PNP Complexes: Synthesis, Characterization and Catalytic Assessment for Base-Free Dehydrogenative Coupling of Alcohols. *Dalton Trans.* **2021**, *50*, 10067–10081; b) Naik, A.; Maji, T.; Reiser, O. Iron(II)-bis(Isonitrile) Complexes: Novel Catalysts in Asymmetric Transfer Hydrogenations of Aromatic and Heteroaromatic Ketones. *Chem. Commun.* **2010**, *46*, 4475; c) De Luca, L.; Mezzetti, A. Base-Free Asymmetric Transfer Hydrogenation of 1,2-Di- and Monoketones Catalyzed by a (NH)<sub>2</sub>P<sub>2</sub>-Macrocyclic Iron(II) Hydride. *Angew. Chem. Int. Ed.* **2017**, *56*, 11949–11953; d) Bigler, R.; Mezzetti, A. Isonitrile Iron(II) Complexes with Chiral N<sub>2</sub>P<sub>2</sub> Macrocycles in the Enantioselective Transfer Hydrogenation of Ketones. *Org. Lett.* **2014**, *16*(24), 6460–6463.
- (9) Patil, P.; Ahmadian-Moghaddama, M.; Dömling, A. *Green Chem.* **2020**, *22*, 6902–6911.

- (10) Yagoub, I.; Clémancey, M.; Bayle, P.-A.; Quintard, A.; Delattre, G.; Blondin, G.; Kochem, A. Mössbauer spectroscopic and computational investigation of an iron cyclopentadienone complex. *Inorg. Chem.* **2021**, *60*, 11192–11199.
- (11) Miyanaga, S.; Yasuda, H.; Sakai, H.; Nakamura, A. Semiconducting organometallics: Electrical conducting behavior of Fe(CO)<sub>3</sub>(diene) doped with iodine and their <sup>57</sup>Fe Mössbauer spectroscopic studies. *Chem. Mat.* **1989**, *1*, 384–390.
- (12) Dias, G. H. M.; Morigaki, M. K. Mössbauer parameters and structure correlations in five-coordinate iron complexes. *Polyhedron* **1992**, *11*, 1629–1636.
- (13) Brougham, D. F.; Barrie, P. J.; Hawkes, G. E.; Abrahams, I.; Motevalli, M.; Brown, D. A.; Long, G. J. Solid state dynamics of tricarbonyl( $\eta^5$ -1,5-cycloheptadienyl)iron tetrafluoroborate. *Inorg. Chem.* **1996**, *35*, 5595–5602.
- (14) Zanello, P.; Herber, R. H.; Kudinov, A. R.; Corsini, M.; Fabrizi de Biani, F.; Nowik, I.; Loginov, D. A.; Vinogradov, M. M.; Shul'pina, L. S.; Ivanov, I. A.; Vologzhanina, A. V. Synthesis, structure, electrochemistry, and Mössbauer effect studies of (ring)Fe complexes (ring = Cp, Cp\*, and C<sub>6</sub>H<sub>7</sub>). Photochemical replacement of benzene in the hexadienyl complex [( $\eta^5$ -C<sub>6</sub>H<sub>7</sub>)Fe( $\eta$ -C<sub>6</sub>H<sub>6</sub>)]<sup>+</sup>. *J. Organomet. Chem.* **2009**, *694*, 1161–1171.
- (15) See ref 6a and a) Emayavaramban, B.; Chakraborty, P.; Dahiya, P.; Sundararaju, B. Iron-Catalyzed  $\alpha$ -Methylation of Ketones Using Methanol as the C1 Source under Photoirradiation. *Org. Lett.* **2022**, *24*, 6219–6223. b) Abdallah, M.-S.; Joly, N.; Gaillard, S.; Poater, A.; Renaud, J.-L. Blue-Light-Induced Iron-Catalyzed  $\alpha$ -Alkylation of Ketones. *Org. Lett.* **2022**, *24*, 5584–5589; c) Waheed, M.; Alsharif, M. A.; Issa Alahmdi, M.; Mukhtar, S.; Parveen, H. Visible Light Promoted Iron-Catalyzed One-Pot Synthesis of 2-Arylimino-2H-Chromenes from 2-Hydroxybenzyl Alcohols and  $\beta$ -Ketothioamides at Room Temperature. *Eur. J. Org. Chem.* **2023**, e202300136.
- (16) See 3a-b, g and: a) Roudier, M.; Constantieux, T.; Rodriguez, J.; Quintard, A. Recent achievements in enantioselective borrowing hydrogen by the combination of iron- and organo-catalysis. *Chimia.* **2016**, *70*, 97–101; b) Quintard, A. Development of Multicatalytic Strategies Based on the Combination between Iron-/Copper- and Organo-catalysis. *Isr. J. Chem.* **2021**, *61*, 278–288. For the similar approach combining two metals, see: c) Lichosyt, D.; Zhang, Y.; Hurej, K.; Dydio, P. Dual-catalytic transition metal systems for functionalization of unreactive sites of molecules. *Nature Catalysis* **2019**, *2*, 114–122; d) Zhang, X.; Ma, W.; Zhang, J.; Tang, W.; Xue, D.; Xiao, J.; Sun, H.; Wang, C. Asymmetric Ruthenium-Catalyzed Hydroalkylation of Racemic Allylic Alcohols for the Synthesis of Chiral Amino Acid Derivatives. *Angew. Chem. Int. Ed.* **2022**, *61*, e202203244; e) Chang, X.; Cheng, X.; Liu, X.; Fu, C.; Wang, W.; Wang, C. Stereodivergent Construction of 1,4-Nonadjacent Stereocenters via Hydroalkylation of Racemic Allylic Alcohols Enabled by Copper/Ruthenium Relay Catalysis. *Angew. Chem. Int. Ed.* **2022**, *61*, e202206517.
- (17) See ref 10 and Werley, B. K.; Hou, X.; Bertonazzi, E. P.; Chianese, A.; Funk, T. W. Substituent Effects and Mechanistic Insights on the Catalytic Activities of (Tetraarylcyclopentadienone)iron Carbonyl Compounds in Transfer Hydrogenations and Dehydrogenations. *Organometallics* **2023**, *42*, 3053.

# TOC

